

ОБЪЕДИНЕННЫЙ
ИНСТИТУТ
ЯДЕРНЫХ
ИССЛЕДОВАНИЙ

Дубна

E17-96-316

B.Brutovsky¹, M.Hnatic², D.Horvath³, M.Stehlik³

SCALE-INVARIANT FORM
OF TURBULENT VISCOSITY
IN UNIVERSAL TURBULENCE DECAY MODEL

Submitted to «Journal de Physique, II»

¹P.J.Šafarik University, Košice, Slovakia

²Permanent address: Institute of Experimental Physics, SAS, Košice, Slovakia

³Institute of Experimental Physics, Slovak Academy of Sciences, Košice, Slovakia

Брутовски Б. и др.
 Скейлинговая форма турбулентной вязкости
 в модели универсальной распадной турбулентности

Рассмотрена модель сильно развитой турбулентности в бесконечной пространственной области. Изучаемые потоки предполагаются изотропными, однородными, несжимаемыми, диссипативными и распадающимися из полностью хаотического состояния. Продолжен анализ [L.Ts.Adzhemyan et al., Preprint P17-94-319, Dubna, 1994; Czech. J. Phys., vol.45 (1995) p.517] распадной турбулентности, в которой спектр кинетической энергии и функция переноса выражены через скейлинговую функцию $\bar{F}(kl_K)$ в энергосодержащей области. Ее безразмерный аргумент является произведением зависящей от времени длины Кармана $l_K(t)$ и волнового числа k . При больших k скейлинговая функция имеет колмогоровскую асимптотику $k^{-5/3}$ с инфракрасной поправкой $\mathcal{O}(k^{-7/3})$. Было показано, что численно найденная функция $\bar{F}(kl_K)$ позволяет определить скейлинговую форму турбулентной вязкости типа Гейзенберга. Предложен также численный метод для исследования области малых аргументов функции \bar{F} , где вычислительные трудности становятся существенными.

Работа выполнена в Лаборатории теоретической физики им. Н.Н.Боголюбова ОИЯИ.

Препринт Объединенного института ядерных исследований. Дубна, 1996

Brutovsky B. et al.
 Scale-Invariant Form of Turbulent Viscosity in Universal Turbulence Decay Model

The strongly developed turbulence in an infinite spatial domain is considered. Studied flows are assumed to be isotropic, homogeneous, incompressible, dissipative and decaying from the fully chaotic state. We have extended the analysis [L.Ts.Adzhemyan et al., Preprint P17-94-319, Dubna, 1994; Czech. J. Phys., vol.45 (1995) p.517] of the turbulence decay, where the kinetic energy spectrum and the mean transfer are expressed by means of scaling function $\bar{F}(kl_K)$ in energy containing region. Here dimensionless argument is the product of time-dependent Kármán length $l_K(t)$ and wave number k . The scaling function tends to have the Kolmogorov $k^{-5/3}$ asymptotics with $\mathcal{O}(k^{-7/3})$ infrared correction for large k . We have shown that approximatively computed function $\bar{F}(kl_K)$ allows to find the scaling form of turbulent viscosity of the Heisenberg type. Moreover, a method for the investigation of the region of small \bar{F} arguments where the numerical difficulties become significant is suggested.

The investigation has been performed at the Bogoliubov Laboratory of Theoretical Physics, JINR.

1 Introduction

To describe the large scale statistics of turbulence, many phenomenological or so-called engineering closure models have been constructed. Their principal feature is the use of empirically estimated constant parameters. Recently great attention has been devoted to a deeper and more fundamental understanding of the turbulence essence and to the calculation of the above mentioned empirical constants.

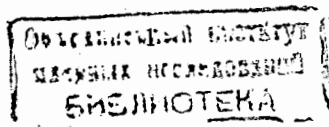
Fundamental statistical turbulence theories are prevalingly based upon the Navier - Stokes equation or its modifications. The strong nonlinearity of Navier-Stokes equation at sufficiently high Reynolds numbers is responsible for the standard closure problem of the statistical turbulence theory. The important quantity present in the classical phenomenological models (e.g. in the basic Reynold's stress model for the evolution of the mean large scale velocity field) is the turbulent viscosity ν_T . The ways of its determination are ambiguous. In the present work the attention is focussed onto the classical Heisenberg type turbulent viscosity [1].

In the original Heisenberg's theory the phenomenological closure $T(k, t) \sim [E(k, t)]^{\frac{3}{2}}$ is introduced which associates the mean energy transfer $T(k, t)$ with the energy spectrum $E(k, t)$. Instead of, we have applied a more fundamental form of statistical closure mediated by the scaling function \tilde{F} . This function of dimensionless argument $kl_k(t)$ (l_k being the characteristic length scale) is completely determined with the universal turbulence decay model [2], formulated on the base of renormalization group theory results. Note that the renormalization group methods, applied for the first time to the turbulence theory within the framework of the model of randomly forced Navier-Stokes equation [3, 4, 5] belong to wide-spread approaches to describe the developed turbulence.

In accordance with Refs. [2, 6] the core of the scale-invariant theory consists in the presence of the time dependent characteristic length scale $l_k(t)$. The conclusions of above outlined theory have demonstrated its responsibility to valuable contribution to the explanation of past grid experiments summarized in [6]. In present paper the following qualitatively new theoretical and computational aspects appear: i) the application of non-traditional numerical technique to find the solution of systems of integro-differential equations determining the form of \tilde{F} ; ii) the method of calculation of Heisenberg type turbulent viscosity as well as connected measurable universal constant parameter as an important consequence of the model.

2 Self - similar description of turbulence decay process

One of the primary purposes of the present paper is to show the continuity between the recently developed model of universal turbulence decay [2] and the standard closure models. Before discussing the consequences of the modified turbulent viscosity model we will display the main results and recapitulate the salient points of the



analysis [2].

It must be emphasized that the considerations are valid for the energy containing scales and for very large Reynolds numbers under the condition that the principal single independent scale of the system (von Kármán scale) [7]

$$l_k = \left(\frac{2}{d} \mathcal{E} \right)^{\frac{2}{3}} \varepsilon^{-1} \quad (1)$$

(where \mathcal{E} and ε are the mean kinetic energy and the energy dissipation rate, respectively) is much larger than the mean size of dissipation micro-eddies.

The second order statistics of turbulence decay process can be characterized by means of non stationary $E(k, t)$ spectrum

$$E(k, t) = \frac{S_d k^{d-1}}{2(2\pi)^d} \int d^d \mathbf{r} \exp[-i\mathbf{k} \cdot \mathbf{r}] \langle v_j(\mathbf{x}, t) v_j(\mathbf{x} + \mathbf{r}, t) \rangle \quad (2)$$

In this equation, $v_j(\mathbf{x}, t)$ is velocity field, d is the spatial dimension, $S_d = 2\pi^{\frac{d}{2}}/\Gamma[\frac{d}{2}]$ is the surface of a d -dimensional sphere, Γ denotes Gamma function and brackets $\langle \dots \rangle$ denote the statistical averaging over the \mathbf{v} field realizations.

The derivation of the governing equations for the scaling function \tilde{F} starts with the assumption that $E(k, t)$ can be written in the scaling form

$$E(k, t) = \dot{V}_{rm}^2(t) l_k(t) \frac{C_k}{d} \chi^2 \tilde{F}(\chi), \quad \chi \equiv kl_k(t), \quad (3)$$

where C_k is Kolmogorov constant and the root of mean square velocity

$$V_{rm}(t) = \sqrt{\langle [v_j(\mathbf{x}, t) v_j(\mathbf{x}, t)] \rangle}$$

is connected with the energy spectrum by relation

$$\frac{V_{rm}^2(t)}{2} = \int_0^\infty dk E(k, t). \quad (4)$$

The scaling idea of Ref. [6] comprises the supposition that $l_k(t)$, $V_{rm}(t)$, $\mathcal{E}(t)$, $\varepsilon(t)$ and Reynolds number $Re_l(t)$ undergo the following time dependencies

$$\begin{aligned} l_k(t) &= l_k(t_c) \left(\frac{t}{t_c} \right)^{\frac{2}{3}}, & V_{rm}(t) &= V_{rm}(t_c) \left(\frac{t}{t_c} \right)^{-\frac{3}{5}}, \\ \mathcal{E}(t) &= \frac{1}{2} V_{rm}^2(t_c) \left(\frac{t}{t_c} \right)^{-\frac{8}{3}}, & \varepsilon(t) &= \frac{3}{5} V_{rm}^2(t_c) \left(\frac{t}{t_c} \right)^{-\frac{11}{5}}, \\ V_{rm}(t_c) &= \frac{3 d^{\frac{3}{2}} l_k(t_c)}{5 t_c}, & Re_l(t) &= \frac{l_k(t) V_{rm}(t)}{\nu}, \end{aligned} \quad (5)$$

where $t_c, l_k(t_c), V_{rm}(t_c)$ are integration constants, ν is the kinematic viscosity. The universal decay dynamics (3) can occur only during the finite time interval [6].

According to Ref. [2] the results of perturbative renormalization group theory can be adapted for the description of the states located near the statistical equilibrium - fully developed and stationary turbulent regime. Then the mean energy transfer [7] defined as

$$T(k, t) = \frac{S_d k^{d-1}}{(2\pi)^d} \int d^d \mathbf{r} \exp[-i\mathbf{k} \cdot \mathbf{r}] \langle v_s(\mathbf{x}, t) v_j(\mathbf{x} + \mathbf{r}, t) \frac{\partial}{\partial r_j} v_s(\mathbf{x} + \mathbf{r}, t) \rangle \quad (6)$$

can be rewritten into the scaling form

$$T(k, t) = C_k^{\frac{3}{2}} \varepsilon(t) l_k(t) \left(\frac{2Q^{(d)}}{3d} \right) I^{(d)}[\chi; \langle \tilde{F} | \tilde{F} \rangle], \quad (7)$$

where $Q^{(d)}$ parameter is

$$Q^{(d)} = \frac{3 d S_{d-1}}{2(d-1)^{\frac{3}{2}}} \sqrt{\frac{g_*^{(d)}}{(2\pi)^d S_d}} = 2 \sqrt{\frac{3}{\pi}} \frac{d \sqrt{d+2}}{(d-1)^2} \frac{\Gamma[\frac{d}{2}]}{\Gamma[\frac{d-1}{2}]} \quad (8)$$

The value of the parameter $g_*^{(d)}$, ($d > 2$, d is the spatial dimension) appearing in (8) has been fixed by the RNG theory [5]

$$g_*^{(d)} = \frac{8(d+2)(4\pi)^{\frac{d}{2}} \Gamma(\frac{d}{2})}{3(d-1)} \quad (9)$$

in the frame of analytical regularization scheme. At the present stage of RNG theory, the perturbative analysis has been carried out up to one loop order of diagrammatic expansion. The understanding of formula (7) needs to define the bilinear functional form $I^{(d)}[\cdot]$:

$$\begin{aligned} I^{(d)}[\chi; \langle A|B \rangle] &= \chi^{\frac{12}{5}} \int_0^\infty dq \int_0^\pi d\theta K^{(0,d)}(q, \theta) \\ &\times \left\{ K^{(1,d)}(q, \theta) A(\chi q) B(\chi p) + K^{(2,d)}(q, \theta) A(\chi q) B(\chi) \right. \\ &\left. + K^{(3,d)}(q, \theta) A(\chi p) B(\chi) \right\}, \end{aligned} \quad (10)$$

where $p(q, \theta) = \sqrt{1 - 2q \cos \theta + q^2}$, $A(\cdot)$ and $B(\cdot)$ are two arbitrary functions of single variable and the integral kernels

$$\begin{aligned} K^{(0,d)}(q, \theta) &= \frac{(\sin \theta)^d}{p^2} \frac{1}{1 + q^{\frac{2}{3}} + p^{\frac{2}{3}}}, \\ K^{(1,d)}(q, \theta) &= p^{3-d} q^2 [d - 1 - 2dq \cos \theta + 2(d-2)q^2 + 4q^2 \cos^2 \theta], \\ K^{(2,d)}(q, \theta) &= q^2 [(1-d)p^2 + 2q^2(1 - q \cos \theta)], \\ K^{(3,d)}(q, \theta) &= p^{3-d} q^d [2p^2 \cos \theta + (1-d)q] \end{aligned}$$

are the functions of the rescaled internal momentum.

The scaling forms (3) and (7) connected by the mean energy balance equation [7]

$$\frac{\partial E(k, t)}{\partial t} = T(k, t) \quad (11)$$

are the basis of the self - similar description of the decay process for the scales where the viscous effects are negligible ($\nu \rightarrow 0$). The system of equations determining \tilde{F} and C_k -important measurable parameter

$$\chi^3 \frac{d\tilde{F}}{d\chi} = \sqrt{C_k} Q^{(d)} I^{(d)}[\chi; \langle \tilde{F} | \tilde{F} \rangle], \quad (12)$$

$$\frac{2C_k}{d} \int_0^\infty dx x^2 \tilde{F}(x) = 1 \quad (13)$$

has been derived using (3), (5), (7), (12), (13) and the integral identity (4). The inner structure of equations (12) and (13), supplemented by the asymptotical conditions

$$\begin{aligned} \chi^{\frac{11}{3}} \tilde{F}(\chi) &= 1 + \mathcal{O}(\chi^{-\frac{2}{3}}), \quad \text{for } \chi \rightarrow \infty, \\ \tilde{F}(\chi) &= \mathcal{O}(1), \quad \text{for } \chi \rightarrow 0, \end{aligned} \quad (14)$$

makes the calculation of $\tilde{F}(\chi)$ difficult. The difficulties of the numerical treatment come from the following related aspects of the constructed model: the equations are quadratic in \tilde{F} , contain nonlocal terms and combinations of derivatives and integrals over \tilde{F} . To examine these equations we introduce an approximative method, where the explicit $\tilde{F}(\chi)$ dependence is expressed through "particular spectral objects". From this point the investigation of (12), (13) and (14), we are going to perform, is restricted by the proposed linear parametrization (Sect. 4.), which enables to apply an optimization method (Sect. 5.).

3 The model of turbulent viscosity

There are a few definitions of the turbulent viscosity. In this work Heisenberg's definition was used [1]:

$$\nu_T(k, t) = -\frac{\int_0^k dq T(q, t)}{2 \int_0^k dq q^2 E(q, t)}. \quad (15)$$

Taking into account (3), (11) and (15) we have derived the scaling form of the turbulent viscosity

$$\nu_T(k, t) = \nu \text{Re}_1(t) C_\mu(\chi) \frac{d^{\frac{3}{2}}}{4} = C_\mu(\chi) \frac{\mathcal{E}^2(t)}{\varepsilon(t)}, \quad (16)$$

where

$$C_\mu(\chi) = \frac{4}{3d^3} \left[\frac{3 \int_0^\chi dx x^2 \tilde{F}(x) - \chi^3 \tilde{F}(\chi)}{\int_0^\chi dx x^4 \tilde{F}(x)} \right]. \quad (17)$$

From the connection $\varepsilon(t) = 2\nu \int_0^\infty dk k^2 E(k, t)$ [1] and relations (11) and (15) follows that the turbulent viscosity of very small scales

$$\nu_T(\infty, t) = -[\varepsilon(t)]^{-1} \nu \int_0^\infty dk T(k, t) \quad (18)$$

is equal to ν , which is zero order quantity at the energy containing scales.

The form of (16) has been chosen to be compatible with so-called $k - \varepsilon$ model (see [8, 9]) where

$$\nu_T = C_\mu(0) \frac{\mathcal{E}^2}{\varepsilon}. \quad (19)$$

It is obvious that (16) can be considered as a generalization of (19) for the turbulent decay statistics using χ dependent C_μ instead of constant one. The Eq. (16) can be also viewed as a rough analogue of the equation used in the kinetic theory of molecular gases. If the inertial eddies are taken as "molecules" with the characteristic mean free path l_K , zero diameter and mean collision frequency $V_{rm}(t)/l_K$, then the kinematic viscosity of such a "gas" is given by the expression $\nu_T(t) \sim V_{rm}(t)l_K(t)$ obtained from (19).

4 The linear parametrization of the scaling function

The explicit form of the linear parametrization of \tilde{F} is proposed:

$$\tilde{F}(\chi) = \sum_{J=1}^n b_J \phi_J(\chi) - h_{AS} \sum_{J=1}^n w_J \psi_J(\chi), \quad (20)$$

where the functions ϕ_J, ψ_J were chosen in the form

$$\begin{aligned} \phi_1(\chi) &= [\chi^2 + \mu_\phi^2]^{-\frac{11}{6}}, & \psi_1(\chi) &= \chi^2 [\chi^2 + \mu_\psi^2]^{-\frac{19}{6}}, \\ \phi_J(\chi) &= \mathcal{N}_J^\phi \phi_1(\chi) \chi^{J-2} e^{-\frac{\chi}{2\mu_\phi}}, & \psi_J(\chi) &= \mathcal{N}_J^\psi \psi_1(\chi) \chi^{J-2} e^{-\frac{\chi}{2\mu_\psi}}, \end{aligned} \quad (21)$$

$$\mu_\phi = 1.7, \quad \mu_\psi = 5.3, \quad 2 \leq J \leq n$$

and calibration conditions are given by

$$b_1 = w_1 = 1. \quad (22)$$

The leading terms of \tilde{F} of the order $\mathcal{O}(\chi^{-\frac{11}{3}})$ and $\mathcal{O}(\chi^{-\frac{13}{3}})$ coming only from $\phi_1(\chi)$, $\psi_1(\chi)$ functions are responsible for the conservation of the Kolmogorov $k^{-\frac{5}{3}}$ behaviour and its $k^{-\frac{7}{3}}$ infrared correction (3) in the limit of large wavenumbers $k \gg l_K^{-1}$.

The normalization parameters \mathcal{N}_J^ϕ , \mathcal{N}_J^ψ and parameters Y^ϕ , Y^ψ are defined by integral conditions

$$\begin{aligned} \int_0^\infty dx x^2 \phi_{J \geq 2}(x) &= \int_0^\infty dx x^2 \phi_1(x) = Y^\phi, \\ \int_0^\infty dx x^2 \psi_{J \geq 2}(x) &= \int_0^\infty dx x^2 \psi_1(x) = Y^\psi. \end{aligned} \quad (23)$$

The motivation for the selection of linear \tilde{F} parametrization in b_J , w_J , h_{AS} is to separate the numerical and optimizational stages to make the solution of the equations less time consuming.

Using (14) we obtain the asymptotical expansion of the left (lhs(χ)) and right hand side (rhs(χ)) of (12):

$$\begin{aligned} \text{lhs}(\chi) &= -\frac{11}{3} \chi^{-\frac{5}{3}} + \mathcal{O}(\chi^{-\frac{7}{3}}) \\ \text{rhs}(\chi) &= -h_{AS} \sqrt{C_k} Q^{(d)} I_\infty^{(d)} \chi^{-\frac{5}{3}} + \mathcal{O}(\chi^{-\frac{7}{3}}), \end{aligned} \quad (24)$$

where $I_\infty^{(d)} \equiv I^{(d)}[\chi; \langle \tilde{F} | \tilde{F} \rangle]_{\chi \rightarrow \infty}$. The equating of the amplitudes corresponding to $\mathcal{O}(\chi^{-\frac{5}{3}})$ asymptotics gives

$$h_{AS} = \frac{11}{3 \sqrt{C_k} Q^{(d)} I_\infty^{(d)}}. \quad (25)$$

Taking into account (13), (20) and (23) the Kolmogorov constant

$$C_k = \frac{\frac{d}{2}}{Y^\phi \sum_{J=1}^n b_J - h_{AS} Y^\psi \sum_{J=1}^n w_J} \quad (26)$$

can be expressed by means of the representation

$$[b, w] \equiv (b_1, b_2, b_3, \dots, b_n, w_1, w_2, \dots, w_n,) \quad (27)$$

From (25) and (26) we obtain the explicit expression

$$C_k = \left(\frac{c_a + \sqrt{c_a^2 + c_b^2}}{2 c_b} \right)^2, \quad (28)$$

where

$$c_a = \frac{2}{d} Y^\phi \sum_{J=1}^n b_J, \quad c_b = \frac{22 Y^\psi \sum_{J=1}^n w_J}{3 d Q^{(d)} I_\infty^{(d)}}. \quad (29)$$

Substituting (20) into (12) the equation for spectral balance can be rewritten as

$$\begin{aligned} \sum_{J=1}^n b_J \mathcal{D}_J^\phi(\chi) - h_{AS} \sum_{J=1}^n w_J \mathcal{D}_J^\psi(\chi) &= \sqrt{C_k} Q^{(d)} \\ \times \sum_{K,J=1}^n \left\{ b_K b_J I^{(d)}[\chi; \langle \phi_K | \phi_J \rangle] \right. \\ - h_{AS} b_K w_J (I^{(d)}[\chi; \langle \phi_K | \psi_J \rangle] + I^{(d)}[\chi; \langle \psi_J | \phi_K \rangle]) \\ \left. + h_{AS}^2 w_K w_J I^{(d)}[\chi; \langle \psi_K | \psi_J \rangle] \right\} + \Delta(\chi), \end{aligned} \quad (30)$$

where we denote

$$\mathcal{D}_J^\phi(\chi) \equiv \chi^3 \frac{d\phi_J}{d\chi}, \quad \mathcal{D}_J^\psi(\chi) \equiv \chi^3 \frac{d\psi_J}{d\chi}. \quad (31)$$

It can be expected that (30) is not satisfied for any *ad hoc* class of ϕ_J , ψ_J functions and $[b, w]$ parameters. In the large χ region, the connection (25) guarantees the suppression of $\Delta(\chi)$ deviation [since $\Delta(\chi) \equiv \text{lhs}(\chi) - \text{rhs}(\chi) \rightarrow \mathcal{O}(\chi^{-\frac{7}{3}})$]. For the suitable functions ϕ_J and ψ_J the satisfactory enough minimization of errors $\Delta(\chi_m)$ at each point of the nonuniformly distributed mesh χ_m , $m = 1, 2, \dots, \text{mesh}$ can be achieved by finding the appropriate values of $[b, w]$ parameters.

The advantage of the above mentioned separation of the numerical and optimization parts is that many times repeated $\Delta(\chi)$ evaluations (Sect.5) require only a single numerical calculation of each matrix element

$$\begin{aligned} I^{(d)}[\chi_m; \langle \varphi_K(\chi_m \dots) | \varphi_J(\chi_m \dots) \rangle], & \quad I^{(d)}[\chi_m; \langle \varphi_K(\chi_m \dots) | \psi_J(\chi_m \dots) \rangle], \\ I^{(d)}[\chi_m; \langle \psi_K(\chi_m \dots) | \varphi_J(\chi_m \dots) \rangle], & \quad I^{(d)}[\chi_m; \langle \psi_K(\chi_m \dots) | \psi_J(\chi_m \dots) \rangle]. \end{aligned}$$

From the parametrization (21) it follows that the Taylor expansion of \tilde{F} around the zero of χ contains the term of the order $\mathcal{O}(\chi)$. Consequently the lowest order of ν_T [see Eq.(17)] is proportional to $(1/\chi)(b_2 - 2b_3\mu_\phi\mathcal{N}_3^\phi/\mathcal{N}_2^\phi)$ as $\chi \rightarrow 0$. Assuming the special type of relation

$$b_2 = b_3 \frac{2\mu_\phi\mathcal{N}_3^\phi}{\mathcal{N}_2^\phi}. \quad (32)$$

this singularity can be removed and the substitution of (21) and (32) into (20) gives a finite value

$$C_\mu(0) = \frac{12h_{AS}\mu_\phi^{\frac{17}{3}}(1+w_2\mathcal{N}_2^\psi) + \mu_\psi^{\frac{19}{3}}(22+47\mu_\phi b_3\mathcal{N}_3^\phi - 12\mu_\phi^2 b_4\mathcal{N}_4^\phi)}{\frac{9d^2}{2}\mu_\phi^2\mu_\psi^{\frac{19}{3}}(1+2\mu_\phi b_3\mathcal{N}_3^\phi)}. \quad (33)$$

5 Determination of scaling function

The optimum approximative scaling function $\tilde{F}(\chi)$ (given by the set of $[b, w]$ parameters) must satisfy (30) with as small $\Delta(\chi)$ as possible. In our work the determination of the corresponding $[b, w]$ set was carried out as the multiparameter optimization procedure over the $[b, w]$ parameter space. The aim of the optimization was to find the set of $[b, w]$ providing the minimum value of some functional constructed from $\Delta(\chi)$.

To find the optimum parameter set the Genetic Algorithm (GA) approach [10, 11] was applied, having been claimed to be a robust global optimization technique over poorly understood nonlinear parameter spaces [12, 13].

The GA mimics the evolution of biological species. The most salient features of the GA are the encoding of a parameter set (i.e. a point in the parameter space) on the string over the low cardinality alphabet (the most often binary) and using the population of the strings instead of the only point. The initial population of the points is randomly generated, all the following populations (next generations) are created by means of genetic-like operators (mutation, recombination and survival of the fittest) from the previous one. As it was shown [10, 11], the search is gradually biased to the most promising partitions of the parameter space during the optimization process.

Objective function. Success of the GA used as the function optimizer crucially depends on the appropriate definition of the objective function expressing the validity of the parameter set. Generally, the task GA solves consists in the search for the set of parameters providing the minimum (or maximum) value of the objective function.

In our case the objective function represents the above mentioned conveniently defined functional constructed from the $\Delta(\chi)$.

The equation (30) was investigated in the mesh points $\chi_m, m = 1, 2, \dots, mesh = 112$. The distribution of the mesh points was given by

$$\chi_m = \begin{cases} \chi_{m-1} + 0.1, & m = 1, 2 \dots 19 \\ \chi_{m-1} + 0.3, & m = 20, 21 \dots mesh \end{cases} \quad (34)$$

where $\chi_0 = 0.1$.

For further purposes, the value of left hand side of (30) in the m -th mesh point is denoted as lhs_m and the term rhs_m represents $lhs_m - \Delta(\chi_m)$. The definition of the objective function Of was based on the lhs_m and rhs_m values and it was taken as the multiplication of the parts Of_1, Of_2 and Of_3 .

Of_1 represented the most significant criterion based on the root mean square deviation between the lhs_m and $rhs_m, m = 1, 2 \dots mesh$:

$$Of_1 = \sqrt{\frac{1}{mesh} \sum_{m=1}^{mesh} \left(\frac{(\chi_m - \chi_{m-1}) |lhs_m - rhs_m|}{0.1 + \frac{|lhs_m - lhs_{m-1}|}{\chi_m - \chi_{m-1}}} \right)^2}, \quad (35)$$

where $mesh$ is the number of the mesh points. To weaken the influence of the deviations in the steep parts of the left hand side of (30) on the Of_1 value, each of the deviation between the lhs_m and rhs_m was divided by the numerical derivation of the left hand side of (30) in the corresponding mesh point. Of_2 provided gentle bias of the optimization procedure to the partitions of the parameter space resulting in good agreement between the minimum $lhs_m, m = 1, 2 \dots mesh$ value and minimum $rhs_m, m = 1, 2 \dots mesh$ value denoted as $Min\{lhs_m\}$ and $Min\{rhs_m\}$, respectively:

$$Of_2 = 1 + 0.1(1 + gen) |Min\{lhs_m\} - Min\{rhs_m\}| \quad (36)$$

Of_2 was generation-dependent as it contained the current generation number (gen parameter).

To push out the strings representing the parameter sets providing positive rhs_m values (which do not seem to be probable) from the population, the third partial objective function Of_3 was defined as:

$$Of_3 = 1 + 0.05 N_{rhs}, \quad (37)$$

N_{rhs} being the number of mesh points in which $rhs_m > 0$.

As it was mentioned above, the total objective function consisted of the three partial objective functions taken multiplicatively:

$$Of = Of_1 \cdot Of_2 \cdot Of_3. \quad (38)$$

Selection scheme. In GA theory, selection scheme represents the reflection of the objective function value of the string in the number of its offspring. For our purposes, *fitness* value was constructed for each string on the base of its objective function value using the *monotonic assignment function*. The number of offspring was proportional to its fitness value.

The following assignment function was used:

$$fitness_i = \begin{cases} 1 & \text{if } Of < threshold \\ \exp \left\{ - \left[\frac{N - bett - rank_i}{0.5(N - bett)} \right]^2 \right\} & \text{otherwise} \end{cases}$$

where N is the population size, $rank_i$ is the rank of the i -th string according to its Of value (the rank of the string with the highest Of value is 0), and the parameter $bett$ is the number of the strings with $Of < threshold$ in the corresponding generation.

As only the rank of the string according to its objective function value appears in the assignment function (instead of the objective function value itself), the applied selection scheme is the type of ranking [14].

The threshold function was *ad hoc* defined:

$$threshold = 10^3 \exp \left(-\frac{gen}{10} \right) + \exp \left(-\frac{gen}{75} \right) \quad (39)$$

where gen is the current generation number.

The reason we have introduced the threshold strategy was to lower the probability of the *premature convergence* [11], i.e. being stuck in the local optimum in $[b, w]$ space. At first, the equity of the convergence into many local optima is kept by the high threshold value. As the search proceeds, lowering of the threshold values forces GA to focus on fewer and fewer local optima. We assume that the application of the threshold strategy has enhanced the exploration phase. Nevertheless, more exact assessment of the influence of the threshold strategy on the GA optimization and its comparison with the other GA-alternatives have not been carried out yet.

Parameters of applied GA procedure. The generational Gray coded [15] GA was applied, 32 bits per parameter (as a result, each parameter set was represented by $32 \times 13 = 416$ bits long string), the standard 2-point crossing over [11], the population size of 10000 strings and mutation rate 1 per 1000 bits. $[b, w]$ (except b_1, w_1 and b_2) were restricted to the grid values:

$$\begin{aligned} b: & -0.5, -0.5 + H_B, -0.5 + 2H_B, \dots, 0.5 - 2H_B, 0.5 - H_B, 0.5 \\ w: & -1.0, -1.0 + H_W, -1.0 + 2H_W, \dots, 1.0 - 2H_W, 1.0 - H_W, 1.0. \end{aligned}$$

where $H_B = 2^{-32}$ and $H_W = 2^{-31}$. The b_1 and w_1 were kept equal to 1.0, b_2 was calculated using Eq.(32).

Gradual decreasing of the objective function value during the optimization procedure is depicted in Fig.1.

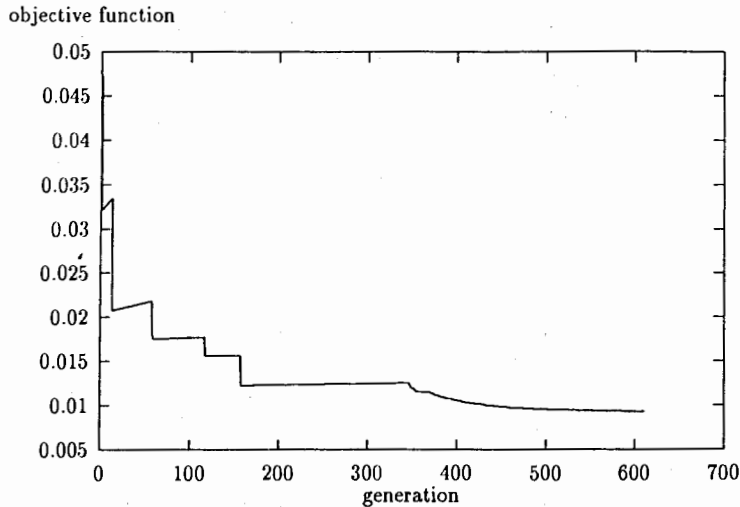


Fig.1. The best achieved objective function value vs. generation.

As a result of the optimization procedure the set of $[b, w]$ parameters providing

the minimum Of value was achieved:

$$\begin{aligned} b_2 &= 6.15447702741973010^{-2}, & w_2 &= -2.57404933510675310^{-1} \\ b_3 &= 5.01292772940661010^{-2}, & w_3 &= -8.33162716085362010^{-1} \\ b_4 &= -1.76859040902196210^{-1}, & w_4 &= -3.32600752667663810^{-1} \\ b_5 &= 6.02334650606460610^{-2}, & w_5 &= -1.02254231717031010^{-1} \\ b_6 &= 5.38767086234587910^{-2}, & w_6 &= -3.80170521647709110^{-1} \\ b_7 &= -6.04551705905364810^{-2}, & w_7 &= 9.89421240750099810^{-2} \\ b_8 &= 2.57542940149443010^{-2}, & w_8 &= -3.30607159373026110^{-1}. \end{aligned} \quad (40)$$

Hamming distance. This metrics [16] is used to express the similarity of two binary strings. It is equal to the number of distinct bits in the corresponding positions. Hamming distance shows the convergence properties of the GA optimization procedure.

In our work only the 8 most significant bits out of 32 total bits per parameter were included into Hamming distance. The average Hamming distance of the two strings in the randomly generated initial population is 52 (4×13).

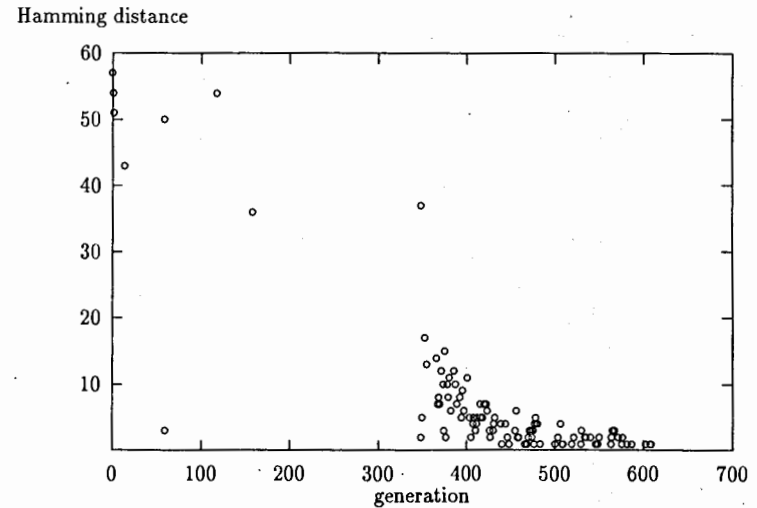


Fig.2. Hamming distance between the string providing the lowest Of value and the previous best string. It can be seen that the Hamming distance decreases with the number of generations. In the end, the variations between the strings are very small meaning that the population has converged and the improvements of the Of value are negligible.

6 The calculation of the velocity skewness

It is interesting to calculate the so-called skewness factor $S(r, t)$ with an obvious definition

$$S(r, t) = \frac{\langle [[v_j(\mathbf{x} + \mathbf{r}, t) - v_j(\mathbf{x}, t)] r_j]^3 \rangle}{\langle [[v_j(\mathbf{x} + \mathbf{r}, t) - v_j(\mathbf{x}, t)] r_j]^2 \rangle^{3/2}}. \quad (41)$$

From the supposition that $E(k, t)$ and $T(k, t)$ are of specific scaling behaviour [6] follows the scaling form of the averaged squared and cubed finite differences $[v_j(\mathbf{x} + \mathbf{r}, t) - v_j(\mathbf{x}, t)]r_j$. Thus we can introduce the functions

$$f_n(\xi) = \frac{\langle [[v_j(\mathbf{x} + \mathbf{r}, t) - v_j(\mathbf{x}, t)] r_j]^n \rangle}{V_{in}^n(t)} \quad \text{as } n = 2, 3. \quad (42)$$

The dimensionless parameter $\xi = r/l_k(t)$ represents a separation distance of point $\mathbf{x} + \mathbf{r}$, \mathbf{x} in the Kármán units. Using the standard procedures, aiming to connect the \mathbf{x} and wavenumber representations, it is possible to connect $f_2(\xi)$ and $f_3(\xi)$ functions with $\tilde{F}(\chi)$ via the convolutions

$$f_n(\xi) = \xi^{n-5} \int_0^\infty dy K_n(y) \tilde{F}\left(\frac{y}{\xi}\right) \quad (43)$$

with the integral kernels

$$K_2(y) = \frac{2C_k y^2}{3} \left(\frac{2}{3} - K_E(y) \right), \quad K_3(y) = -\frac{4C_k}{3^{5/2}} \frac{d}{dy} [y^2 K_E(y)] \quad (44)$$

containing

$$K_E(y) = \left(1 + \frac{d^2}{dy^2} \right) \frac{\sin y}{y}. \quad (45)$$

The skewness factor (41) can be expressed as

$$S(r, t) = S(\xi l_k(t), 1) = \frac{f_3(\xi)}{f_2^{3/2}(\xi)}. \quad (46)$$

In Fig.3. we present $S(r, t)$ dependence as a function of ξ calculated using relations (43), (44), (45) and (46).

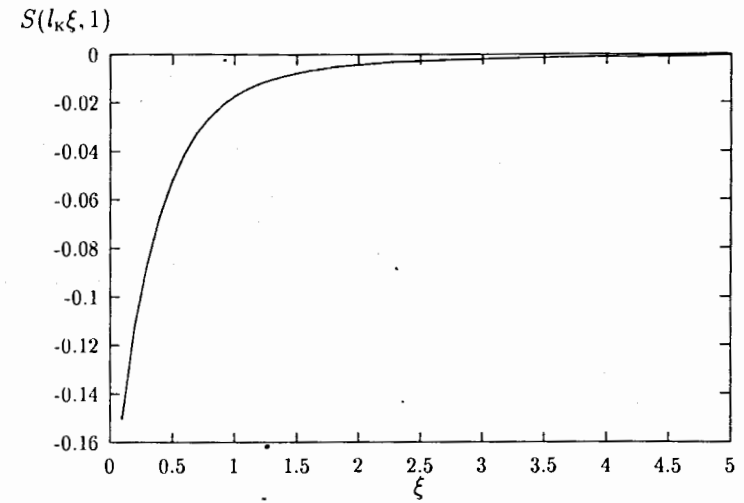


Fig.3. Skewness factor as a function of dimensionless ξ variable

7 The results of numerical analysis

The set of $[b, w]$ parameters was found by the numeric optimization (Sect. 5). Substituting (40) into (20) the scaling function $\tilde{F}(kl_k)$ has been constructed (Fig.4.). The sum of terms $-h_{AS} \sum_{j=1}^n w_j \psi_j(\chi)$ of the scaling function $\tilde{F}(\chi)$ shows the asymptotic behaviour $\chi^{-13/3}$ as $\chi \rightarrow \infty$ (Fig.5). Substitution of the scaling function (20) with the set of parameters (40) into Eq.(30) gives satisfactory agreement of its right and left hand sides (Fig.6) and corresponding $C_\mu(\chi)$ dependence (Fig.7). Using the equations (33), (25) and (26) with the set of parameters (40) substituted, the values of principal constants have been calculated: $C_k = 1.615$, $h_{AS} = 0.634$, $C_\mu(0) = 0.068$, $S(0, t) = -0.218$. These predictions are close to the empirical values $C_\mu(0) = 0.09$ [8] and $S(0, t) = -0.45$ [1].

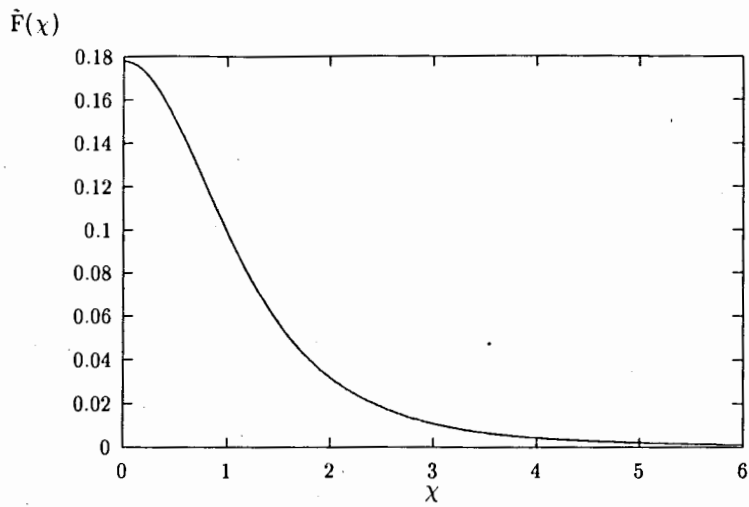


Fig.4. Figure shows the behaviour of the scaling function $\hat{F}(x)$

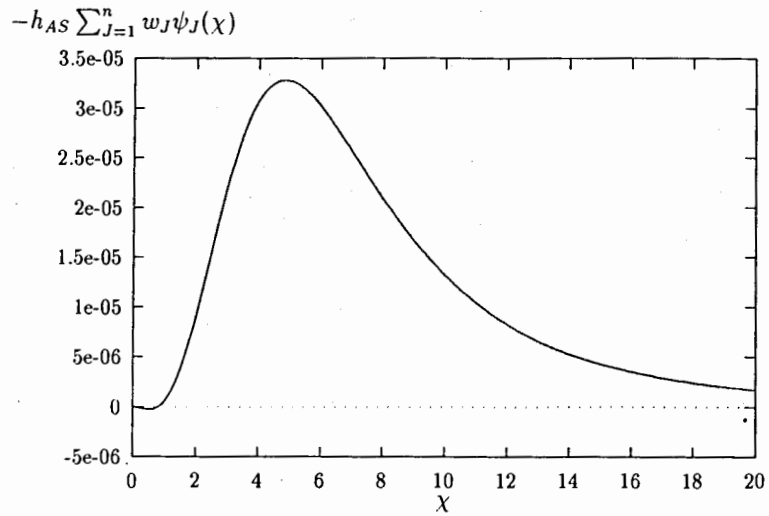


Fig. 5. Figure shows the sum of the terms of the order $O(x^{-13/3})$ included in \hat{F} .

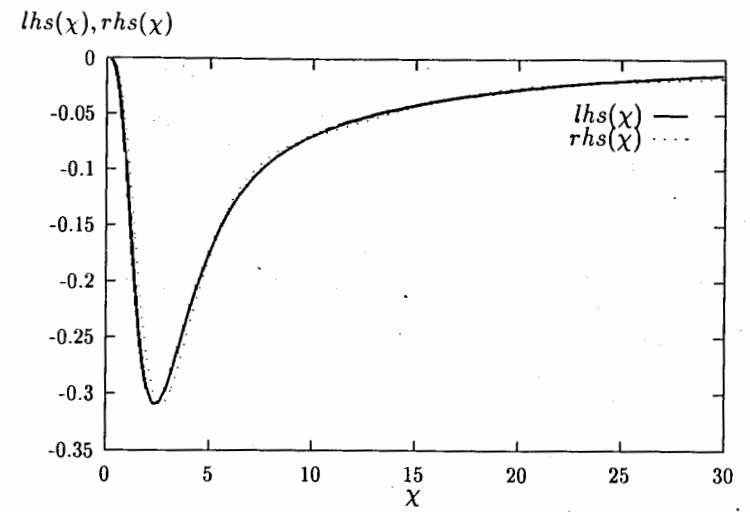


Fig.6. Comparison of the left $lhs(x)$ and right $rhs(x)$ hand sides of Eq. (12).

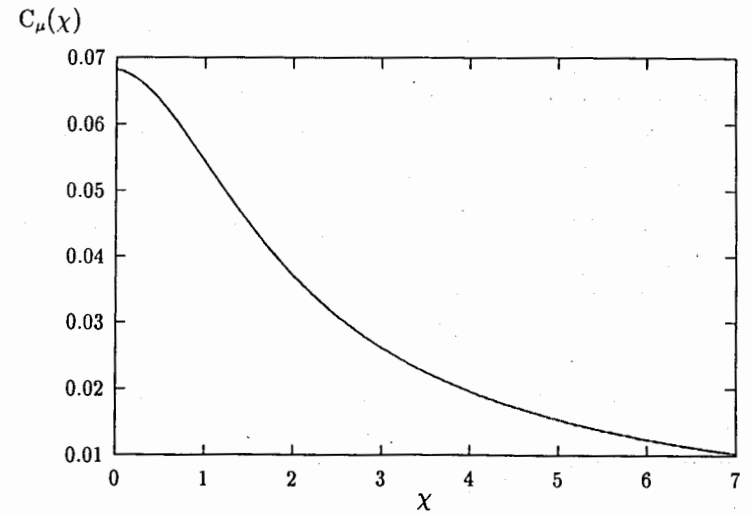


Fig.7. The $C_\mu(x)$ dependence calculated from Eq.(17).

8 Single stationary large scale vortex decay in the frame of Reynolds stress model for mean velocity field

The separation of scales between the mean and fluctuating fields is based on Kolmogorov's concept that turbulence is more isotropic and homogeneous at small scales. The simplest classical closure model approximating the strongly turbulent Navier-Stokes dynamics at very large scales is the Reynolds stress model

$$\frac{\partial U_i}{\partial t} + U_j \frac{\partial U_i}{\partial x_j} = -\frac{\partial P}{\partial x_i} + \nu \Delta U_i + \frac{\partial \mathcal{R}_{ij}}{\partial x_j} \quad (47)$$

with the continuity equation

$$\frac{\partial U_j}{\partial x_j} = 0, \quad (48)$$

where \mathcal{R}_{ij} is the Reynolds stress, U_i is the component of mean velocity field, P is the mean pressure. In the first order modelling, the simple eddy-viscosity representation (Bussinesq approximation) of the Reynolds stress [9] is given by

$$\mathcal{R}_{ij} = -\frac{2}{3} \varepsilon \delta_{ij} + \nu_T \left(\frac{\partial U_i}{\partial x_j} + \frac{\partial U_j}{\partial x_i} \right). \quad (49)$$

We assume that strongly turbulent structures create the background of single large eddy and the turbulence of scales, less or comparable with the length l_K , is statistically homogeneous whereas the inhomogeneities are of the typical size of $\infty \gg R \gg l_K$.

To describe the evolution of the background fluctuations we have employed the model non-equilibrium turbulent viscosity [see Eq. (16)]:

$$\nu_T(0, t) = C_\mu(0) \frac{\mathcal{E}^2(t)}{\varepsilon(t)}. \quad (50)$$

After its embedding into incompressible Reynolds stress model (47) and (48) a combined model emerges, which can be investigated for various geometries. As we are planning to study the single vortex (with fixed center position) in the infinite spatial domain (unbounded problem) it is convenient to suppose the cylindrical symmetry. Assuming that

$$\mathbf{U} \equiv U_\varphi(R, t) \mathbf{e}_\varphi, \quad P \equiv \text{constant}, \quad (51)$$

(where R is a distance from the eddy center and \mathbf{e}_φ is unit polar vector) the continuity equation $\partial U_\varphi / \partial \varphi = 0$ is satisfied automatically, large scale non linearity vanishes

$$(\mathbf{U} \cdot \nabla) \mathbf{U} = \frac{U_\varphi}{R} \frac{\partial \mathbf{U}}{\partial \varphi} = 0$$

and with the help of (50) the equation (47) can be replaced by

$$\frac{\partial U_\varphi(R, t)}{\partial t} = \nu_T(0, t) \hat{\Delta}_R U_\varphi(R, t), \quad \text{with Laplacian} \quad \hat{\Delta}_R = \frac{1}{R} \frac{\partial}{\partial R} \left(R \frac{\partial}{\partial R} \right). \quad (52)$$

Assuming the special property

$$U_\varphi(R, t) = v_{rm}(t) \bar{\Phi}(\bar{\eta}), \quad \bar{\eta} = \frac{R}{l_K(t)}, \quad (53)$$

(where $\bar{\Phi}$ is some continuous function of single variable $\bar{\eta}$) the substitution of (53) into (52) gives

$$\frac{dv_{rm}(t)}{dt} \bar{\Phi}(\bar{\eta}) - \frac{v_{rm}(t)}{l_K(t)} \frac{dl_K(t)}{dt} \bar{\eta} \bar{\Phi}(\bar{\eta}) = \frac{\nu_T(t) v_{rm}(t)}{l_K^2(t)} \hat{\Delta}_{\bar{\eta}} \bar{\Phi}(\bar{\eta}). \quad (54)$$

Taking into account the time dependences in (5) complete time and scale $\bar{\eta}$ separation is possible in Eq. (54) and the following equation can be derived:

$$\bar{\Phi}(\eta) + \frac{2}{3} \eta \frac{d\bar{\Phi}(\eta)}{d\eta} + \hat{\Delta}_\eta \bar{\Phi}(\eta) = 0; \quad \eta = \bar{\eta} \sqrt{\frac{3l_K^2(t_c)}{5t_c \nu_T(t_c)}}, \quad \bar{\Phi}(\eta) \equiv \bar{\Phi}(\bar{\eta}), \quad (55)$$

which connects only the η -dependent quantities. We have investigated the problem (55) in limit case of large η ratio. The solution of this differential equation can be expressed in the form of asymptotical series. The evolution of the $U_\varphi(R, t)$ in the region distant enough from the eddy center ($R \gg l_K$), where the inhomogeneity of the turbulence is smaller than near to the core of eddy is described by

$$\bar{\Phi}(\eta) = \Phi_\infty \eta^{-\frac{3}{2}} \left(1 + \frac{27}{16\eta^2} + \frac{3969}{512\eta^4} + \frac{480249}{8192\eta^6} \right) + \mathcal{O}(\eta^{-\frac{15}{2}}), \quad \text{as } \eta \rightarrow \infty. \quad (56)$$

From the supplementary condition the integration constant Φ_∞ can be determined.

9 Conclusion

In our work the properties of "self similar solutions" of decay turbulence spectrum have been investigated. The presented method combines the analytical and numerical approaches. It has been shown that variational formulation and consequent multi-path optimization strategy can provide information about the solution of nonlocal and nonlinear problems. Acceptable values of the Kolmogorov constant, skewness factor and also constant included in the formula for turbulent viscosity have been obtained.

M.Hnatic is grateful to D.I.Kazakov and to director D.V.Shirkov for hospitality at the Laboratory of Theoretical Physics, JINR, Dubna. This work was supported by Slovak Grant agency for science (grant 2/550/96).

References

- [1] W.D. McComb. *The Physics of Fluid Turbulence*. Clarendon Press Oxford, 1990.
- [2] L. Ts. Adzhemyan and M. Hnatich and M. Stehlik. Renormgrupovoj rascot spektrov zatuchajuscej turbulentnosti v energosoderzhascej i inercionnoj oblasti. Technical Report P17-94-319, Joint Institute for Nuclear Research, Dubna, 1994.
- [3] D. Forster and D.R. Nelson and M.J. Stephen. Large-distance and long - time properties of a randomly stirred fluid. *Phys. Rev. A*, 28:1000, 1977.
- [4] C. DeDominicis and P. C. Martin. Energy spectra of certain randomly-stirred fluids. *Phys. Rev. A*, 19:419, 1979.
- [5] L. Ts. Adzemjan and A. N. Vasiljev and J. M. Pismak. RG-podchod k teorii turbulentnosti: Razmernosti sostavnych operatorov. *Teor. i mat. fiz.*, 57(2):268-281, 1983.
- [6] W.M. George. The decay of homogeneous isotropic turbulence. *Phys. Fluids A*, 4:1492, 1992.
- [7] G.K. Batchelor. *The theory of Homogeneous turbulence*. Cambridge, England, 1953.
- [8] B. E. Launder and A. Morse and W. Rodi and D. B. Spalding. Prediction of free shear flows - a comparison of the performance of six turbulence models. In *Free Turbulent Shear Flows, Vol.1, NASA Report No. SP-321*, pages 361-422, 1973.
- [9] V. Yakhot and S. A. Orszag and S. Thangam and T. B. Gatski and C. G. Speziale. *Phys. Fluids A*, 4(7):1510-1520, 1992.
- [10] J. H. Holland. *Adaptation in natural and artificial systems*. MIT Press, 1992.
- [11] D. E. Goldberg. *Genetic algorithms in search, optimization, and machine learning*. Addison-Wesley, 1989.
- [12] D. Whitley. Deception, dominance and implicit parallelism in genetic search. *Annals of Mathematics and Artificial Intelligence*, 5:49-78, 1992.
- [13] S. Forrest. Genetic algorithms: Principles of natural selection applied to computation. *Science*, 261:872-878, 1993.
- [14] D. E. Goldberg and K. Deb. A comparative analysis of selection schemes used in genetic algorithms. In G. J. E. Rawlins, editor, *Foundations of Genetic Algorithms*, pages 69-93, 1991.
- [15] D. E. Goldberg. Real-coded genetic algorithms, virtual alphabets, and blocking. *Complex Systems*, 5:139-167, 1991.
- [16] G. J. E. Rawlins. *Foundations of Genetic Algorithms*, pages 1-11. Morgan Kaufmann Publishers, 1991.

Received by Publishing Department
on August 29, 1996.